Available online at www.sciencedirect.com

ScienceDirect

Energy Procedia 69 (2015) 178 – 187

Energy Procedia

International Conference on Concentrating Solar Power and Chemical Energy Systems, SolarPACES 2014

A holistic approach for low cost heliostat fields

A. Pfahl[a]*, M. Randt[b], F. Meier[c], M. Zaschke[d], C.P.W. Geurts[e], M. Buselmeier[d]

[a]*German Aerospace Center (DLR), Institute of Solar Research, Pfaffenwaldring 38-40, 70569 Stuttgart, Germany*
[b]*TRINAMIC Motion Control GmbH & Co KG, Waterloohain 5, 22769 Hamburg, Germany*
[c]*Hamburg University of Technology, Institute of Telematics (E-17), Schwarzenbergstraße 95, 21073 Hamburg, Germany*
[d]*Wacker Ingenieure – Wind Engineering, Gewerbestraße 2, 75217 Birkenfeld, Germany*
[e]*Netherlands Org. for Applied Scientific Research (TNO), Build Environment and Geosciences, PO Box 49, NL 2600 AA Delft, Netherlands*

Abstract

The AutoR-project takes a holistic approach to reduce the cost of heliostat fields: Wireless control and energy supply enables to use smaller heliostats which need less steel per mirror area (but usually have high wiring cost). A low cost but high efficient drive system is chosen which reduces energy consumption to a minimum amount and leads to low cost for PV cell and energy storage. The usual boundary layer wind tunnels tests for heliostats are proven regarding energy spectra to avoid oversizing of steel structure and drives or failures because of underestimations of the loads. The concepts for wireless control and energy supply, the wind tunnel investigations and the first rim drive heliostat prototype are presented.

Peer review by the scientific conference committee of SolarPACES 2014 under responsibility of PSE AG

Keywords: central receiver; autonomous heliostat; rim drive; wind loads

1. Introduction

An impressing amount of concepts for cost reduction of heliostats were developed so far [1]. From these concepts several promising were combined to a new unique heliostat concept: An autonomous light-weight heliostat with rim drives [2]. It was presented at first at the SolarPACES 2012 conference in Marrakesh. A project was initiated to

* Corresponding author. Tel.: +49 711 6862 479; fax: +49 711 6862 8032.
E-mail address: Andreas.Pfahl@dlr.de

Peer review by the scientific conference committee of SolarPACES 2014 under responsibility of PSE AG
doi:10.1016/j.egypro.2015.03.021

develop this kind of heliostat which started in December 2013. To begin simple a first prototype with only one mirror facet of 8m² was built and first principle tests were done. The basic concepts for wireless energy supply and control were developed and first wind tunnel tests to investigate the matching of the energy spectra with standard spectra of the atmospheric boundary layer were performed.

2. Low cost and efficient drive system

The first prototype of a heliostat with rim drives and horizontal first axis is shown in Fig. 1, left. The moved parts are weight balanced which leads to low energy consumption. This was reached only by the rim drives acting as a counter weight and by a slight shifting of the sandwich mirror facet in the mirror plane. The rims are moved by a simple, but rugged and precise winch wheel cable drive system of high efficiency (Fig. 1, right). Because of the big diameter of the rims precise tracking is achieved and low cost gears and motors can be used.

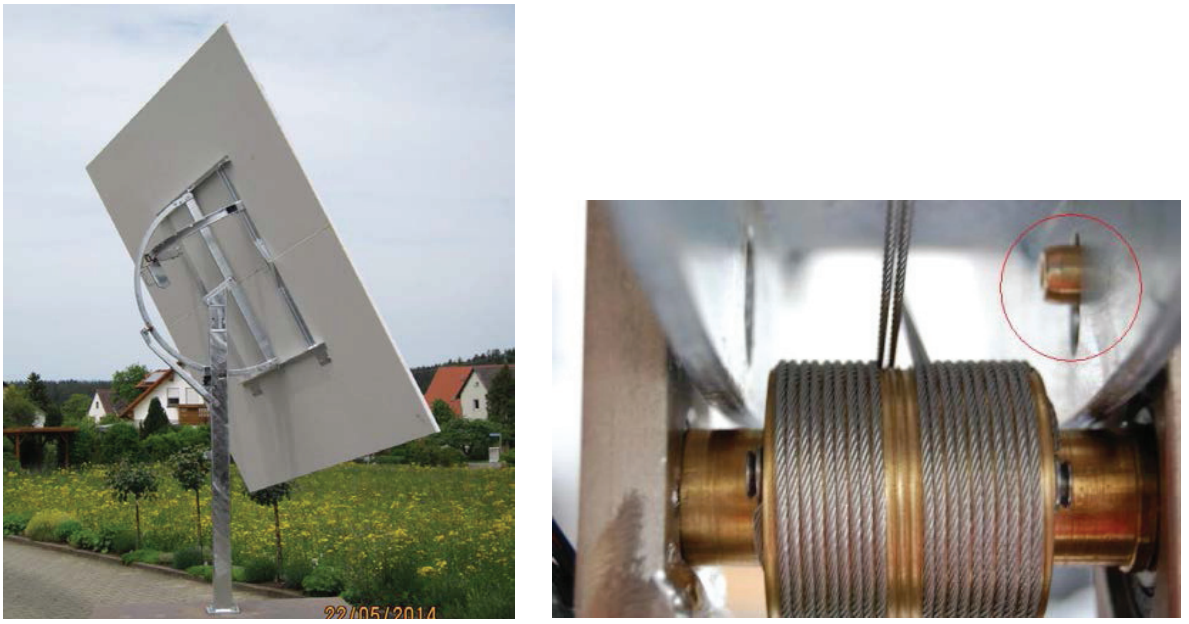

Fig. 1.: Left: First rim drive prototype with 8 m² mirror surface (photo by SOLTEC); Right: Winch wheel cable drive system, locking position of the smaller rim drive. The red circuit shows the extended adjust pin.

To realize the mechanical lock, a low cost linear stepper motor for each rim drive is included. After getting into the stow-position in case of nighttime or emergency, the linear actuators lock the rims and allow the system to stay powerless. A adjust pin which is mounted at the shaft of the linear actuator avoids any movement of the rims. Without the need of a holding current over a long time it provides a higher efficiency than other systems. The locking position of one rim is shown in Fig. 1, right.

First simple tests of the prototype show that the structure is stable and that the winch wheel cable drives and the locking devices work without problems.

3. Wireless energy supply

One major advantage of the concept of the rim drive heliostat is the fact that all components of the drive train have a high efficiency, compared to solutions based on slew drives or lead screw linear actuators. This yields significantly smaller PV-cells – which are used to power the heliostat – as well as batteries or supercaps, which are

locally installed to buffer the energy for emergency moves to stow position or for moves at night, e.g. to move the mirror to cleaning position. The PV panel is dimensioned for sufficient power for tracking in sunny conditions, and to keep the energy buffer device charged, which is again dimensioned to support a certain number of full moves.

The energy harvesting is performed by a photovoltaic panel, supplying power to a battery management / voltage conversion unit which is combined with the battery. The PV cells are operated at the maximum power point and the energy management is handled in a way which ensures maximum life time of the battery, depending on the chosen battery technology. The energy storage and management unit is realized as a smart building block with extensive diagnostic features. The state of health of the battery is permanently analyzed.

The drive control is optimized for low cost as well as for optimum efficiency of the motors, employing a smart sensor system. This closed loop system allows for flexible response concerning wind gusts, as the system's behavior can be programmed.

The electrical system architecture is divided in three parts including PV/wireless for communication and energy sourcing, stepper motor drives for the rim drives control and battery management for energy harvesting. The PV cell is used in maximum power point tracking operation. All units are displayed in Fig. 2.

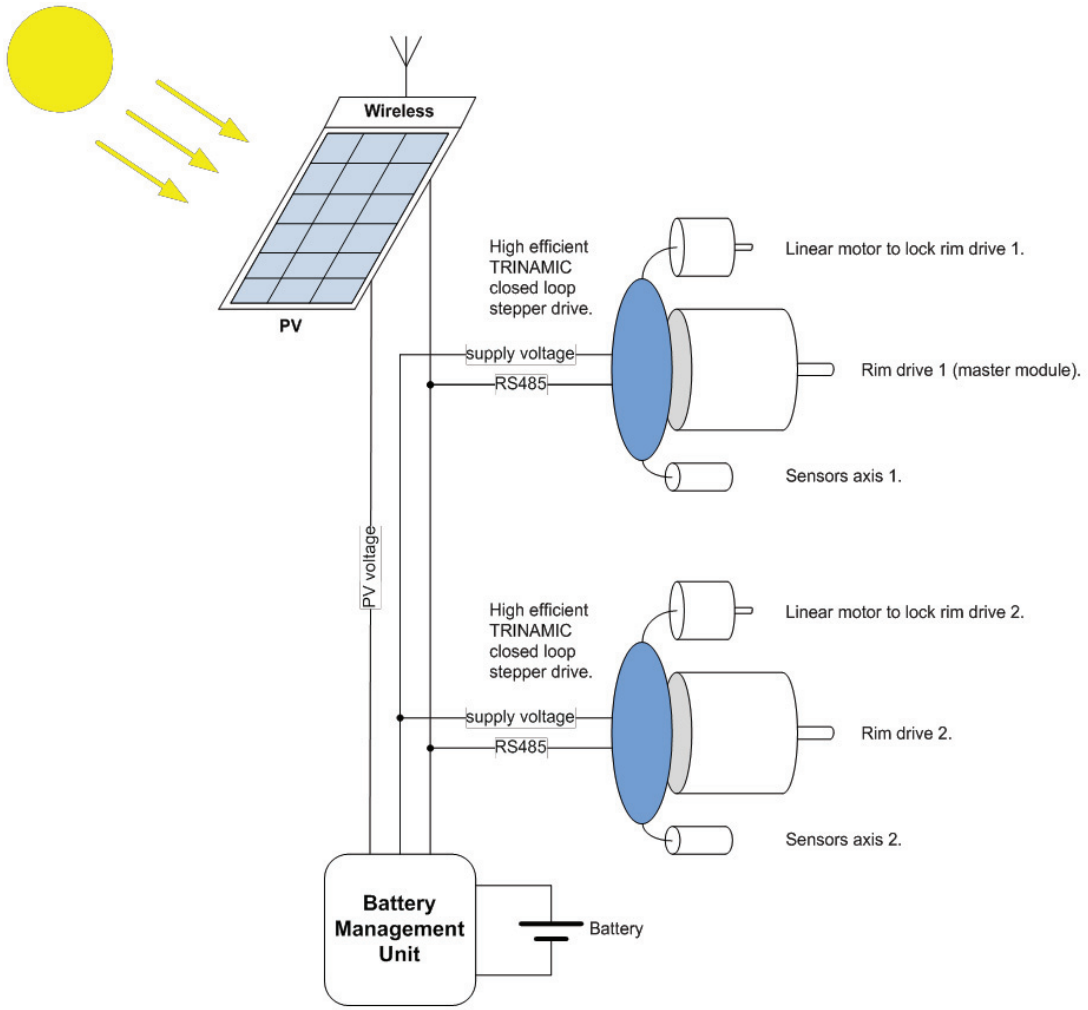

Fig. 2. Rim drive heliostat electrical system architecture.

Due to the high efficiency of the mechanic, a certain amount of energy have to be provided by a battery to continuously maintain the mirror position with the high efficient closed loop drives during wind gusts and cloudy days. To keep the capacity of the energy buffer as small as possible a low power night and emergency mode is implemented. In these modes a mechanical lock (Fig. 2) is applied and all motors are depowered completely to reduce power consumption to minimum.

4. Wireless control

The deployment of a wired fieldbus substantially contributes to the costs of large heliostat fields. They do not only include the material costs of the wires, but also the expenses for trenching, lightning protection and protection against rodents. The estimated wiring cost per heliostat is about $400 for a 20 m² heliostat [3], but they highly depend on the composition of the ground and local regulations. The usage of wireless technology to control the heliostats, together with an autonomous energy supply, eliminates the need for wires and therefore leads to a high cost reduction of the overall plant.

When implementing a wireless control, several issues have to be taken into account. First of all, reliability and real-time capabilities are major requirements for this application to prevent damage and retain efficiency. For example, pump failures or sudden changes of the weather demand for immediate reduction of the irradiated solar energy on the receiver. Losing a corresponding stow signal might lead to disastrous results. Secondly, safety and security threats have to be considered in all stages of the development. Radio waves will not immediately stop at the fences of the plant, so well-tried safety principles have to be applied. Last but not least, the resources needed for supporting such a high number of heliostats in a common concentrated solar power plant are beyond the scope of common wireless systems. The characteristics of a wireless channel, such as problems with simultaneous access to the shared medium, call for an elaborated design of the wireless network and the control application.

In the following, a concept for enabling wireless control of a concentrated solar power plant is presented. It is based on proven standards that are combined and adapted to perfectly fit the needs of such a large wireless control application. Each heliostat is equipped with a low-cost transceiver that transmits according to the IEEE 802.15.4 standard on 2.4 GHz. The transceivers build up a mesh network in which data is forwarded over multiple hops until it reaches the destination. Therefore, a large area can be covered, even with low transmission power and thereby inexpensive hardware. Furthermore, disturbances between distant transceivers are minimized. For authentication of the datagrams, the transceivers contain a hardware security module providing AES-128. The mesh network was already successfully tested at the heliostat field in Jülich [4].

When scaling up the size of the network, it gets increasingly difficult to ensure reliable and timely communication, since the probability of data getting lost rises, because the bandwidth requirement as well as the number of hops increases. We have built a software framework for assessing the capacity of the wireless control network. It can be used to trade-off and optimize the size of the network against data rate and reliability before the deployment. Conventional frameworks for pre-deployment assessment are based on event-based simulators. While they provide certain advantages, such as the possibility to use the same software for hardware and simulation, the results are hard to verify and the simulation takes a long time. Therefore, they are not suitable for very large-scale networks. In contrast, our framework uses an analytical model of the wireless network based on probabilistic modeling. It can therefore assess much larger networks in considerably reduced time of computation (c.f. Fig. 3, right), while the model can be verified much better than a simulation. The left side of Fig. 3 shows an exemplary result of the analytical model. As expected, the reliability of packet delivery decreases with an increase of hops towards the gateway.

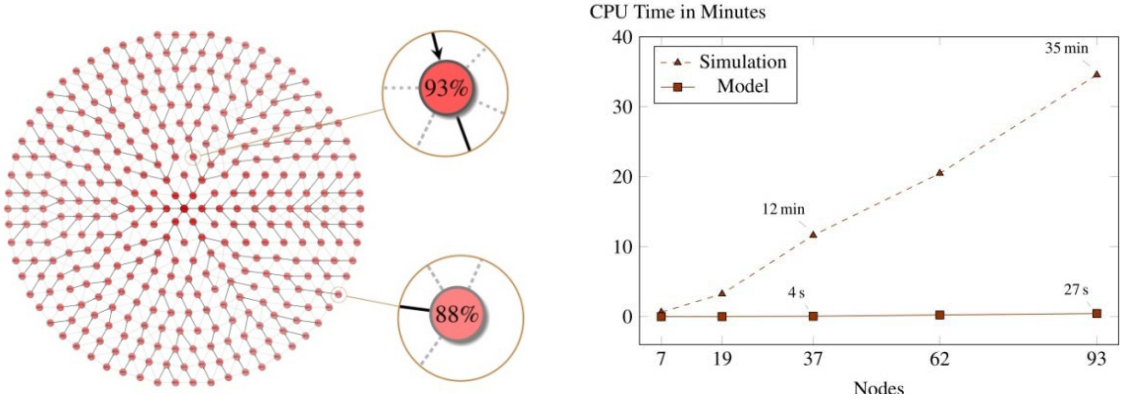

Fig. 3. Left: Depiction of the analytical mode results for a subnetwork of 340 nodes and 10 s packet interval. Right: Comparison of required time for computation for simulation and analytical model.

Because of this, there is a boundary in network size for a given data rate per heliostat. In order to enable even larger networks, a backbone network is advised. For this, the heliostat field is split into several subnetworks. Within each subnetwork, a router is placed that routes between the central field control and the heliostats of the subnetwork. Disturbances between subnetworks can be prevented by choosing different wireless channels. In the easiest case, the gateways are connected via a wired backbone. While this involves the deployment of a wired field bus again, the costs are highly reduced compared to a fully wired solution, since the number of devices connected to the wired field bus is smaller by several orders of magnitude. For a fully wireless solution, the most promising approach is a combination of a virtual backbone as suggested in [5] and a wireless backbone network according to the IEEE 802.11s standard. It is still an open research question, if the required transmission ranges and data rates can be achieved for the fully wireless solution.

Since the size of the subnetworks in particular depends on the data rate, a reduction of the number of datagrams needed to control the heliostats directly decreases the final investment of the plant and is therefore highly advised. In order to unburden the transmission channel from unnecessary transmissions, major parts of the control logic can be moved from the central control into the heliostat itself. For example, together with an appropriate sun position algorithm and an accurate real time clock, the heliostats can autonomously track the sun without external intervention. This keeps the channel free for the essential control commands and reduces the required bandwidth to a fraction of the original bandwidth. Our implementation shows the applicability and usefulness of this approach.

It is furthermore advised to classify the commands according to their reliability and real-time constraints. As introduced previously, emergency signals have to be transmitted reliably within seconds but do not need high data rates and are usually only transmitted from the control station to the heliostats. Other datagrams can tolerate a certain amount of delay, but induce higher bidirectional traffic, such as setting and requesting control parameters or doing firmware updates.

Our approach combines different wireless technologies to tackle the diverging requirements. In addition to the wireless mesh network, a second wireless channel is established to broadcast the emergency signals via an additional long range, unidirectional radio link as depicted on the left side of Fig. 4. It uses a Sub-GHz frequency so it does not interfere with the transmissions in the mesh network. On the right side of Fig. 4, our current hardware prototype for this broadcast channel is shown. The additional cost for utilizing this hardware is marginal, while the gain in reliability and safety is invaluable.

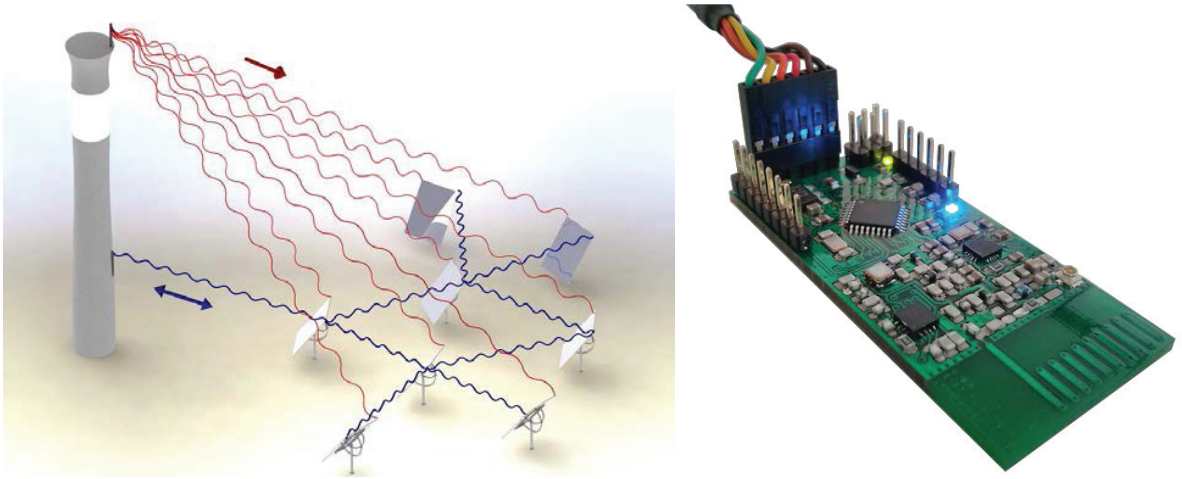

Fig. 4. Left: Dual channel communication system. Right: Prototype for broadcast channel transmitter.

5. Determination of wind loads

Heliostats of central receiver solar power plants are exposed not only to the sun but also to wind. The layout of the foundation, the structure and the drives has to consider the maximal wind loads that are expected to occur. The peak values of the wind load components are highly sensitive to turbulence in the attacking wind. Hence, it is important to model the turbulence of the attacking wind appropriately. A measure for the gustiness of the wind is the turbulence intensity which is the ratio of the standard deviation of the wind speed and the mean wind speed. The turbulence intensity can be measured longitudinal/in the direction of the wind (T_u), lateral/cross-wind in the horizontal plane (T_v) and lateral/cross-wind in the vertical plane (T_w). Accordance of the turbulence intensities alone would not lead to realistic results of wind tunnel tests because not only the total intensity of the gusts is important but also the eddy size distribution. For example, a vortex street behind a cylindrical tube generates eddies of mainly one certain size while in the atmospheric boundary layer a mix of eddies of a wide band width of sizes occurs. At atmospheric boundary layer wind tunnels (BLWT) it is tried to model this mix accordantly. A way to illustrate the distribution of the eddy sizes are the turbulent energy spectra. By Fourier transformation of the signal of wind speed measurement time series the turbulence energy of the flow over the frequency can be calculated. High energy at low frequencies means that big eddies contain much of the energy of the flow while high energy at high frequencies stands for much energy of small turbulence structures (big eddies need a longer time to pass the point of measurement causing a signal of low frequency while small eddies passing quick and causing signals of high frequency). A good matching of the energy spectra means that the turbulence energy of the BLWT is similar distributed over the frequency as in standard atmospheric flow (i.e. the mix of eddy sizes is accordant to full scale).

Recent publications [6] [7] discuss difficulties in matching the turbulence spectrum at measurements of the peak wind loads acting on solar collectors. These are due to the fact that most boundary layer wind tunnels are configured for models at scales of about 1:200 to 1:300, while heliostats need to be modeled at much bigger scales of around 1:10 to 1:20 [8]. At these scales, however, it is usually impossible to meet the scaling requirements regarding turbulence spectra. Due to the limited size of wind tunnels, it is impossible to model large-scale gusts as they are represented in the low-frequency part of the turbulence spectra. The usual way of modeling is to adjust the turbulence intensity at heliostat height to the target value by inserting additional sources of turbulence in the wind tunnel. However, this results necessarily in a falsification of spectra and an accumulation of energy on too high frequencies (i.e. small-scale gusts are disproportionally increased while the large-scale gusts are omitted), see Fig. 5, left. For a match of the turbulence energy at higher frequencies the turbulence intensity would have to be reduced, see Fig. 5, right.

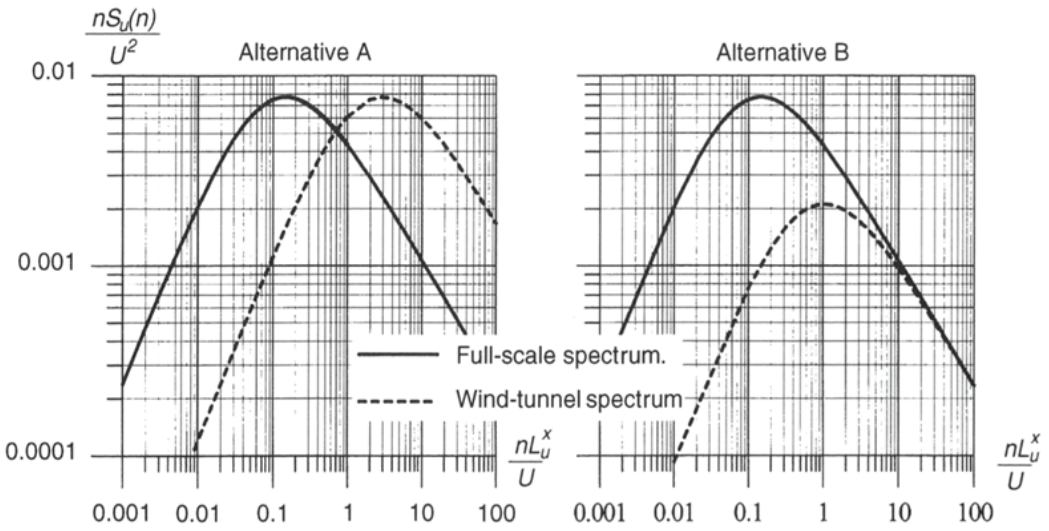

Fig. 5. Left: Matching of turbulence intensity leads to shift of energy to higher turbulence frequencies for big model scales at wind tunnel. Right: Reduced turbulence intensity to reach match of the turbulence energy spectrum at high frequencies. [9]

In order to gain an insight into the relation between heliostat wind loading and turbulence of the approaching flow, wind tunnel tests of a heliostat at stow position with three different turbulence characteristics have been performed. The turbulence characteristics of the approach flow depend on the windward terrain roughness and on the heliostat height. Table 1 illustrates how turbulence intensity decreases with increasing height, i.e. with increasing heliostat size for a typical site (open country with single trees or other obstacles, roughness length z_0=3cm).

Table 1: Elevation axis height and longitudinal turbulence intensities T_u for different heliostat sizes of aspect ratio 1.2 and mirror panel 0.2 m above ground according to [10] (values in brackets extrapolated) for roughness length z_0=3cm.

heliostat size [m²]	8	16	32	64	120
elevation axis height [m]	1.5	2.0	2.8	3.9	5.2
longitudinal turbulence intensity T_u [%]	(21.9)	(20.9)	20.0	19.2	18.6

The horizontal longitudinal turbulence intensities T_u of the three investigated configurations at height of the measurement plate were 21% (BL1), 18% (BL2) and 13% (BL3) (compare Table 2). For these first investigations, the different turbulence conditions were achieved by simply successively removing turbulence generating devices from the boundary layer wind tunnel (see Fig. 6). It was assumed that the shape of the vertical mean wind velocity profile has little effect on the heliostat wind loading (when in stow position) and that the peak wind loads are rather dependent on the approaching turbulence and its spectral properties. Both extensive wind pressure measurements along the upper and lower surface of the heliostat and highly resolved turbulent velocity measurements in the absence of the heliostat have been carried out.

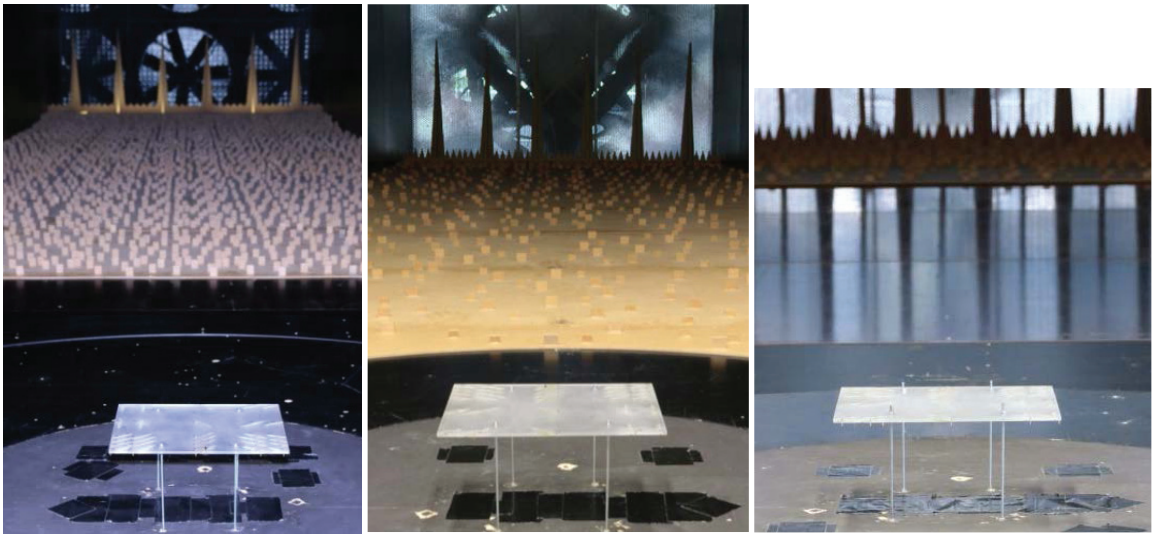

Fig. 6. Spires, fence and roughness elements in wind tunnel to generate boundary layer of 21% (BL1, left), 18% (BL2, middle) and 13% (BL3, right) longitudinal turbulence intensity in height of the heliostat.

The fluctuating graphs of Fig. 7, left, show the energy spectra of BL1 (blue line), BL2 (green line) and BL3 (red line) at a height of 0.12m in BLWT and 2.4m at full scale (assuming a heliostat of 19m², scale 1:20). The frequency (ordinate) is normalized in a way that a value of 1 (10^0) represents eddies/wavelengths approximately of the size of the heliostat chord length. Such eddies can cover the complete heliostat and can have their rotational center in mirror panel height and hence have the highest vertical velocity component attacking the mirror. Eddies between this size and maximal one order of magnitude higher are presumably responsible for the peak loads because smaller eddies do not cover the complete mirror plane and cannot cause high net pressures while bigger eddies have a too small vertical component at mirror panel height. Hence, regarding only the longitudinal energy spectra, they should match especially between values of about 10^{-1} and 10^0 of the normalized frequencies. The dashed lines of Fig. 7 show the standard longitudinal energy spectra of same turbulence intensity T_u. As expected, the energy of the BLWT spectra are shifted towards higher frequencies compared to the full-scale spectra (i.e. the relevant frequencies contain too much energy).

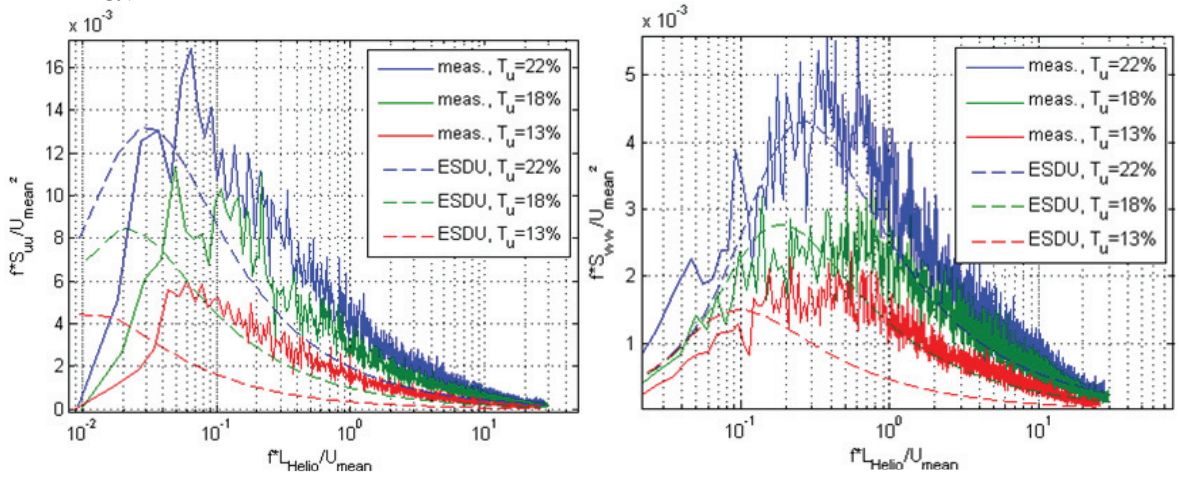

Fig. 7. Left: Longitudinal energy spectra of turbulence. Right: Vertical (lateral) energy spectra of turbulence.

In general, the energy of a flow is proportional to the square of the velocity of the flow. Hence, the turbulent energy of a flow is proportional to the square of the fluctuation of the flow velocity and therefore proportional to the square of the turbulence intensity. Thus, the (dashed) graphs of the standard spectra are related to each other by the factor of the square of the turbulence intensity as can be seen in the graphs. The shift of the peak values of the spectra towards higher frequencies for higher T_u could not be reached in the BLWT tests. It seems that the way of reducing roughness length of these first rough investigations by just reducing the amount of roughness elements reduces the energy of bigger turbulence structures too much.

Since most of the turbulent energy is contained in the longitudinal velocity component and the along-wind gusts are usually dominating the wind loads, it is often sufficient to consider only the longitudinal spectra of turbulence However, for the particular case of a heliostat at stow position, the vertical turbulence component is crucial for the wind forces. For the similar and more general case of a flat plate and the assumption of weak turbulence a linear relation exists between the spectra of lift forces and hinge moment and the energy spectrum of vertical turbulence [11]. This in turn raises the question in how far the high frequency longitudinal spectrum matching approach would be valuable when both turbulence components are relevant. Regarding the vertical spectra (Fig. 7, right) for the relevant frequency band of 10^{-1} to 10^{0} the standard spectra for same longitudinal turbulence intensity match comparably well: A reduction of T_u would lead to too low energy in this band. Only a shift to higher frequencies compared to the standard spectra occurs especially for lower turbulence intensities (similar to the longitudinal energy spectra). Hence, if the vertical velocity component is regarded as decisive for the wind loads at stow position it must be presumed that the common practice of matching the longitudinal turbulence intensity leads to the most realistic results and that a reduction of turbulence intensity would lead to an underestimation of the loads.

Table 2 shows the values of peak lift coefficient and peak hinge moment coefficient obtained from the BLWT tests BL1, BL2 and BL3 with different turbulence intensities at heliostat elevation axis height. The values indicate that there is a pronounced dependency of peak loading on the turbulence of the approach flow. Therefore, it is essential to take the size of heliostats (which is of impact on T_u, compare Table 1) as well as the roughness of the windward terrain into account for the determination of the peak wind loads in stow position.

Table 2: BLWT measurements with different turbulence intensities at height of flat plate.

BLWT configuration	BL1	BL2	BL3
turbulence intensity of longitudinal velocity component [%]	21	18	13
turbulence intensity of vertical velocity component [%]	13	10	8.3
peak lift coefficient	0.59	0.49	0.46
peak hinge moment coefficient	0.20	0.15	0.13

6. Conclusions and outlook

The first tests of the prototype of a heliostat with rim drives and winch wheels of 8m² mirror size showed that the concept works well and is stable under wind load. The heliostat size is not optimized so far. First rough estimations indicate that the cost optimum is reached for 16m² or 32m² (assuming a maximum facet size of 8m²). For smaller plants astigmatism is relevant and hence the smaller size should be used while for big fields astigmatism is of low impact and the bigger size will be most cost effective. The next step will be to measure the tracking accuracy of the first prototype and to build and test a prototype of optimized size.

The energy storage and management unit of the heliostat is realized as a smart building block with extensive diagnostic features and the drive control is optimized for low cost as well as for optimum efficiency of the motors, employing a smart sensor system. When not in operation the heliostat is locked mechanically and the motors can be depowered which reduces power consumption. So all in all, investment and maintenance cost of the system for energy supply is reduced to a minimum.

In order to enable huge wireless mesh networks for heliostat control, the heliostat field is split into several subnetworks and a backbone network is added. In the easiest case, the gateways are connected via a wired backbone. Compared to a full wired solution the costs are highly reduced. For a fully wireless solution, the most

promising approach is a combination of a virtual backbone and a wireless backbone network according to the IEEE 802.11s standard. But it is still an open research question, if the required transmission ranges and data rates can be achieved for the fully wireless solution which demands further research. In addition to the wireless mesh network, a second wireless channel is established to broadcast the emergency signals which leads only to little additional cost but to significantly higher safety and reliability.

The wind tunnel tests showed that further investigations are needed with the aim to "design" the wind turbulence most appropriately by modifications of roughness elements and vortex generators in order to meet the high-frequency spectra matching requirements for the longitudinal and vertical velocity component at once and also regarding the shift of the peak values of the spectra towards higher frequencies for higher turbulence intensities.

In hitherto literature about wind loads on heliostats the impact of heliostat size on the peak wind load coefficients in stow is not accounted for. It is assumed that the wind load coefficients can be used independently of heliostat size. But, by the presented findings it becomes clear that the increase in turbulence intensity of the atmospheric boundary layer for lower heliostat heights leads to significantly higher peak load coefficients for the stow position. Especially in recent years with a trend to smaller heliostats this is getting more important. Hence, wind tunnel investigations with turbulence intensity according to the heliostat size and to the roughness length of the surrounding of the site are mandatory.

The presented wind tunnel investigations will be published soon in more detail in an extra paper.

Acknowledgements

The authors thank the Federal Ministry for Economic Affairs and Energy (BMWi) for its financial support of the project "AutoR" (code 0325629A-C).

References

[1] Pfahl A. Survey of Heliostat Concepts for Cost Reduction, Solar Energy Engineering 2014; 136.
[2] Pfahl A, Randt M, Holze C, Unterschuetz S. Autonomous Light-Weight Heliostat With Rim Drives. Solar Energy 2013; 92, pp 230-240.
[3] Kolb GJ, Jones SA, Donnelly MW, Gorman D, Thomas R, Davenport R, Lumia R. Heliostat Cost Reduction Study. Sandia National Laboratories, Albuquerque, NM, Report No. SAND2007-3293 2007; A.3 p. 103ff and p. 114f.
[4] Kubisch S, Randt M, Buck R, Pfahl A, Unterschütz S. Wireless Heliostat and Control System for Large Self-Powered Heliostat Fields, SolarPACES 2011. Granada, Spain.
[5] Unterschütz S. Methodologies and Protocols for Wireless Communication in Large-Scale, Dense Mesh Networks. PhD Thesis, Hamburg University of Technology, Hamburg, Germany, 2014.
[6] Banks D. Measuring peak wind loads on solar power assemblies. In: Proc. ICWE13 2011. Amsterdam, Netherlands.
[7] Aly AM, Bitsuamlak G. Aerodynamics of ground-mounted solar panels: Test model scale effects. Journal of Wind Engineering and Industrial Aerodynamics 2013; 121, pp 250-260.
[8] Pfahl A, Buselmeier M, Zaschke M. Determination of Wind Loads on Heliostats, SolarPACES 2011. Granada, Spain.
[9] Dyrbye C, Hansen SO. Wind Loads on Structures. Wiley & Sons, Chichester, England, 1997, p 39.
[10] ESDU 85020: Characteristics of Atmospheric Turbulence Near the Ground. Part II: Single-Point Data for Strong Winds (Neutral Atmosphere). Engineering Sciences Data Unit, August 2001.
[11] Rasmussen JT, Hejlesen MM, Larsen A, Walther JH. Discrete Vortex Method Simulations of the Aerodynamic Admittance in Bridge Aerodynamics. J. Wind Eng. Ind. Aerodyn. 2010; 98, pp 754-766.